

Application of the stabilization method to the molecular states of LiHe^{3+} : Energies and radial couplings

A. Macías,* R. Mendizábal, F. Pelayo, A. Riera, and M. Yáñez

Departamento de Química Física y Química Cuántica, Facultad de Ciencias (C-XIV), Universidad Autónoma de Madrid, Cantoblanco, 28049 Madrid, Spain

(Received 23 October 1984)

We have used the stabilization method to perform calculations on autoionizing states of the LiHe^{3+} system which are involved in $\text{Li}^{3+} + \text{He}$ collisions. The molecular energies and radial couplings are calculated with use of programs developed at our laboratory. For both short and large internuclear distances, the stabilization treatment is complemented by block-diagonalization techniques. Our calculations allow us to draw conclusions on the conditions under which these methods can be used to calculate energy positions and radial couplings for states that lie in an ionization continuum.

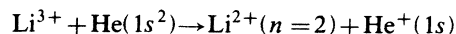
I. INTRODUCTION

In previous work,¹⁻³ we have studied charge-exchange processes that occur in slow and intermediate-energy ion-atom and ion-ion collisions, and which involve the simplest homonuclear (H_2) and heteronuclear (HeH^+) two-electron quasimolecules. The methods of configuration-interaction (CI) and block-diagonalization (BD) were used to calculate the energies of the electronic wave functions in the Born-Oppenheimer approximation and the dynamical couplings between these wave functions. In the present work we extend those studies to the LiHe^{3+} quasimolecule, and we are concerned with the particular molecular states that are involved in a treatment of the electron transfer process $\text{Li}^{3+} + \text{He} \rightarrow \text{Li}^{2+} + \text{He}^+$, for the range $E < 10$ keV/amu of impact energies. The interest of such a process lies in: (a) the series of experiments⁴ which measure the cross section for single electron capture from helium by Li^{3+} ions; (b) its relevance to fusion research, e.g., when Tokamak plasmas are contaminated by Li^{3+} ions; (c) the importance⁵ of charge-exchange processes in the development of short-wavelength lasers; (d) from the theoretical point of view, reported "state-of-the-art" methods in quantum chemistry do not include simultaneous calculations of energies and radial couplings for molecular autoionizing states; (e) the particular technique we choose to calculate these quantities is the stabilization method⁶ because our programs which analytically calculate radial couplings apply directly to this procedure, while for alternative approaches such as the Feshbach projection formalism these programs would require considerable modifications; the basis of the stabilization method has been studied in our group⁷ using the properties of the corresponding Heisenberg transform; and (f) to our knowledge the stabilization method has not been applied to a molecular case; we think it important to show how it can be implemented and to study its advantages and limitations in the calculations of both energies and couplings.

The only theoretical treatments of $\text{Li}^{3+} + \text{He}$ collisions we are aware of have been very recently reported by

Stollberg and Lee,⁸ and Suzuki *et al.*⁹ These calculations envisage the same kind of applications as we do, but employ quite different approaches. Reference 8 employs the Landau-Zener model to calculate estimates of charge-transfer cross sections for He^{2+} and Li^{3+} incident on a series of neutral atoms. For $\text{Li}^{3+} + \text{He}$ collisions, however, their maximum value of the charge-exchange cross section is $\simeq 6 \times 10^{-18}$ cm², for the velocity range $10^7 - 10^8$ cm s⁻¹. Comparison to the data of Wirkner-Bott *et al.*,⁴ which are 100 times larger, indicates that the basic mechanism of the charge-exchange process is not due to transitions taking place at pseudocrossings between the $\text{Li}^{3+} + \text{He}$ and $\text{Li}^{2+}(n=2) + \text{He}^+(1s)$ energy curves. Indeed, the results of Stollberg and Lee⁸ show that these pseudocrossings are traversed diabatically in the impact-energy range considered, and that a detailed molecular treatment is needed to calculate the charge-exchange cross sections. Reference 9 employs the unitarized distorted wave approximation¹⁰ and an independent electron model in which the transferred electron is assumed to move in an average Coulomb potential field with an effective nuclear charge. Their high-energy method,¹¹ however, becomes less reliable at intermediate nuclear energies, and their calculated cross sections lie significantly below the experimental data⁴ in the range $E < 10$ keV/amu.

To treat $\text{Li}^{3+} + \text{He}$ collisions at low energies a molecular expansion of the total wave function representing the colliding system is adequate. Our treatment was carried out in parallel with that of Casaubón *et al.*,¹² who employ a one-electron effective Hamiltonian, assuming that the charge-exchange cross section is dominated by the reaction:



and that one electron remains in a $1s$ orbital of He^{++} throughout the collision and screens the helium nucleus. Since the accuracy of this intuitive approach in representing inner-outer orbital interactions that cause dynamical couplings is not self-evident, it was thought useful to compare their results with those of our *ab initio*

configuration-interaction calculation.

In Sec. II we discuss the main characteristics of the correlation diagram for the molecular states of interest, and in Sec. III we present, and analyze, our results for the molecular energies and radial couplings. Atomic units are used throughout.

II. CORRELATION DIAGRAM

We present in Fig. 1 the qualitative correlation diagram corresponding to the states that strongly interact with the one correlating, at infinite internuclear separation, to the entrance channel $\text{Li}^{3+} + \text{He}(1s^2)$. This diagram has been constructed following the rule of smoothest topological correlation presented in Ref. 13. For the sake of understanding the evolution of the molecular wave functions, we have superimposed on our qualitative diagram the variation, with the internuclear distance, of the molecular orbitals that can be used to describe the corresponding states. In Fig. 1, two molecular orbitals, whose shapes are schematically drawn above and below the corresponding energy line, are then assigned to each state. The basic characteristics of the qualitative diagram are the following: at large internuclear distances the electrons occupy—for the states of interest—either $1s$ orbitals or $2s + 2p$ Stark hybrids; the orbitals delocalize at intermediate internuclear distances and tend to united-atom B^{3+} orbitals at $R = 0$. In some cases, as for the $3d\sigma$ orbital, this is accompanied by a considerable contraction of the electron cloud and there is a promotion effect.¹⁴

The diagram of Fig. 1 can be used to explain why the energies of the molecular states of interest do not correlate to states of the Rydberg series $\text{B}^{3+}(1snl)$ in the united-atom limit. For example, a $1s$ helium orbital can delocalize, yielding either a bonding or an antibonding molecular

orbital, which correlates to a $1s$ and a $2p$ atomic orbital of the united atom, respectively. However, the $1s^2$ and the $1s2p$ states of B^{3+} are already correlated to $\text{Li}^+(1s^2) + \text{He}^{2+}$ and $\text{Li}^{2+}(1s) + \text{He}^+(1s)$, respectively. Hence, by orthogonality, $\text{Li}^{3+} + \text{He}(1s^2)$ must correlate to the $2p^2$ metastable state of the united atom. The same applies to the other states. For example, the state correlating in Fig. 1 to the united-atom $2p3d$ state does so because the corresponding state in the Rydberg series ($1s3d$) is already correlated to $\text{Li}^{2+}(1s) + \text{He}^+(n=2)$, etc.

Figure 1 will be used in the next section to explain the characteristics of the calculated energies and couplings. It may finally be remarked that the fact that all states considered here are autoionizing is only significant at extremely low collision energies. In fact, since their energy widths tend to zero at large internuclear separations, and from the values calculated, e.g., by Sato and Hara¹⁵ together with Z^{-1} expansions for the widths (e.g., Moiseyev and Weinhold,¹⁶ Macías and Riera¹⁷) we can expect that for $v > 0.2$ a.u. collision times are much smaller than ionization lifetimes; at (much) smaller velocities these lifetimes can be introduced in the treatment in a phenomenological way.¹⁸ On the other hand, our molecular description does not include dynamical couplings to ionization channels, whose contribution will become important at velocities greater than 1 a.u.

III. RESULTS AND DISCUSSION

To calculate the energies corresponding to the states indicated in Fig. 1, we have made use of the stability property of the Hamiltonian eigenvalues, which has been reported by Macías *et al.*¹⁹ and will not be repeated here in such detail. Essentially, the method consists in performing a standard CI or BD calculation, and then varying an

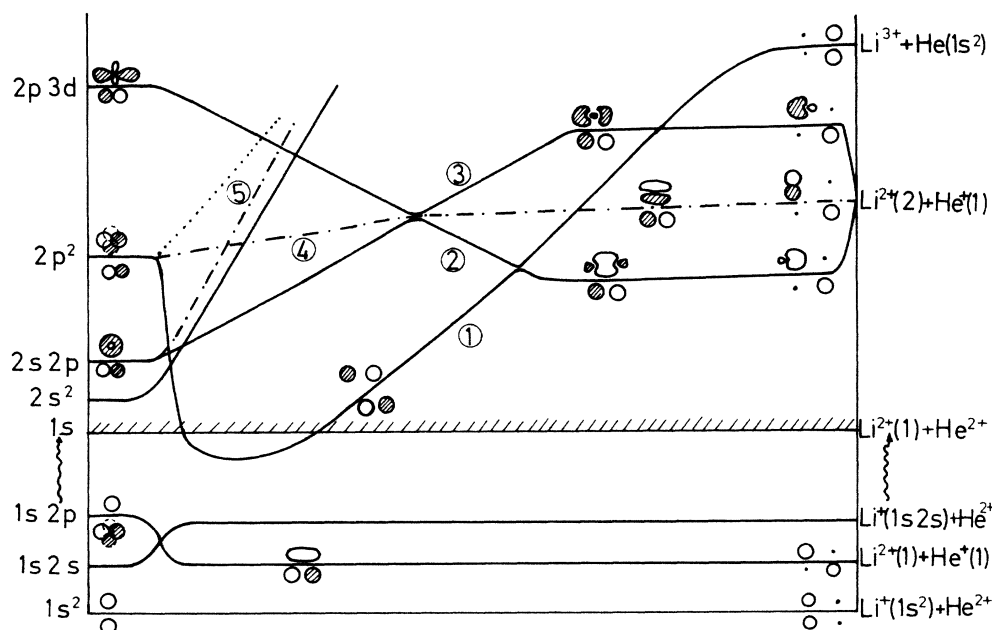


FIG. 1. Qualitative correlation diagram for the metastable states above the ionization limit (hatched line) for the quasimolecule LiHe^{3+} : —, Σ states; - - - - , Π states; · · · · , Δ states.

overall scaling parameter β in the exponents of the Gaussian-type orbitals (GTO's):

$$\phi_{l,m,n,\alpha_i} = N_i x^l y^m z^n \exp(-\alpha_i \beta r^2). \quad (1)$$

The wave functions corresponding to eigenvalues that remain stable and that have the correct physical properties (indicated by the correlation diagram) are then chosen to represent the molecular states. It is worth remarking that, for all states and internuclear distances considered, both conditions were found to be equivalent. That is, stability of eigenvalues always meant that the corresponding wave functions had the correct physical properties, as checked by inspection of the expansion coefficients and vice versa. This is an important point since in all those regions where the character of the wave function is well defined, the stability test of the eigenvalues is unnecessary when using block-diagonalization procedures.¹³

In Figs. 2(a) ($^1\Sigma$ states) and 2(b) ($^1\Pi$ states) we present an illustration of our procedure to check the stability property of the eigenvalues of the molecular Hamiltonian, for a fixed internuclear distance. In Figs. 3 and 4 we

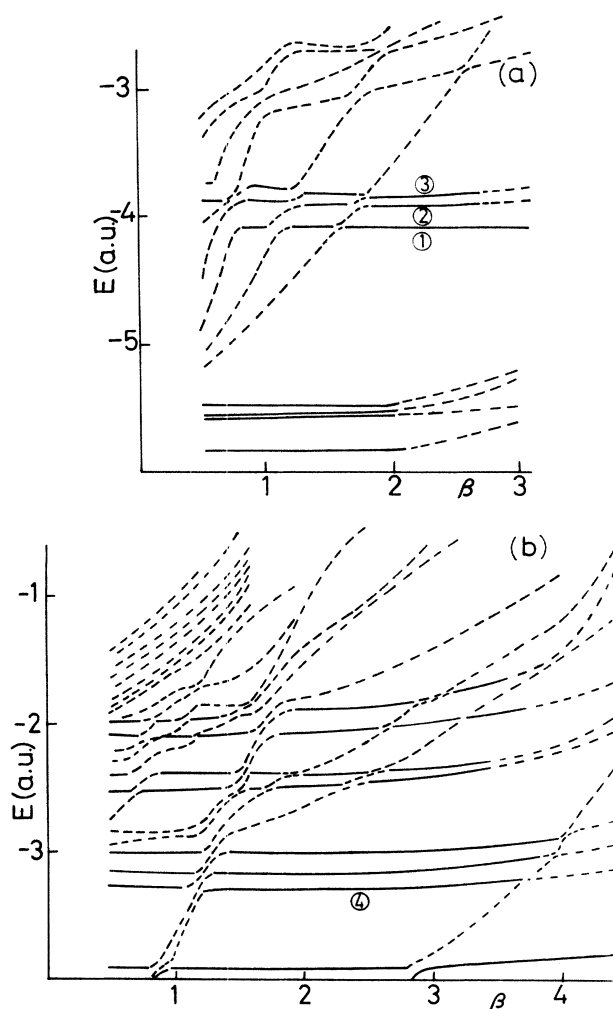


FIG. 2. Stabilization of some eigenvalues of the full CI calculation corresponding to the atomic basis set of Table I, as a function of the scaling parameter β which multiplies all exponents of the GTO's for $R = 5.0$ a.u. (a) Σ states; (b) Π states.

show the behavior of the eigenvalues as functions of both the internuclear distance R and the scaling parameter β of Eq. (1). In both sets of figures stable eigenvalues are shown by full lines and unstable ones by dotted lines. The curves of the stable eigenvalues in Figs. 3 and 4 can then be compared to the qualitative correlation diagram of Fig. 1.

For $0.5 \text{ a.u.} < R < 5 \text{ a.u.}$, we used a full CI approach, where the configurations were built from a two-center basis set of GTO's, given in Table I. For $R > 5 \text{ a.u.}$ and $R < 0.5 \text{ a.u.}$ we have used block-diagonalization procedures, since the character of the wave functions is well defined. More specifically, for $R > 5 \text{ a.u.}$ we have only included in the basis-set configurations of the valence bond (VB) type $\text{Li}^{3+} + \text{He}(nl'n')$ and $\text{Li}^{2+}(n) + \text{He}^+(n'l')$ and used contracted²⁰ GTO's in the atomic basis set (given in Table II) to accurately reproduce $1s$, $2s$, and $2p$ hydrogen-like Li orbitals. For $R < 0.5 \text{ a.u.}$, it proved very convenient to construct diabatic wave functions¹³ of a given molecular orbit (MO) ($2p\sigma^2$, $2s\sigma^2$, etc.) character, by employing an atomic basis set of GTO's (given in Table III)

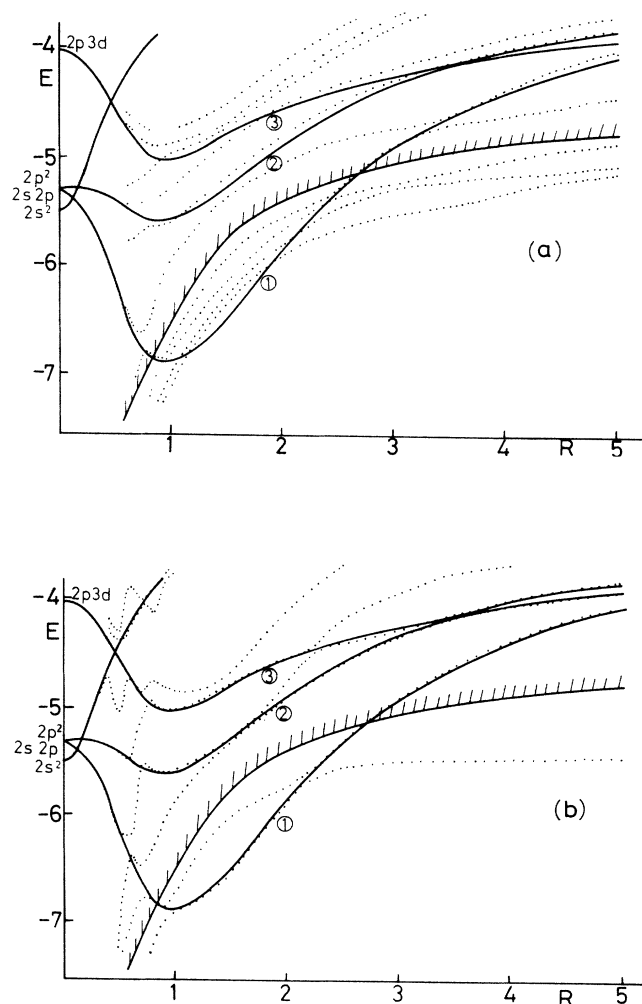


FIG. 3. Stabilization results at intermediate and small internuclear distances for $^1\Sigma$ states. Full lines correspond to stable eigenvalues and the ionization limit is shown. Basis set of Tables I and III. (a) Scaling parameter $\beta = 1.0$; (b) $\beta = 4.0$.

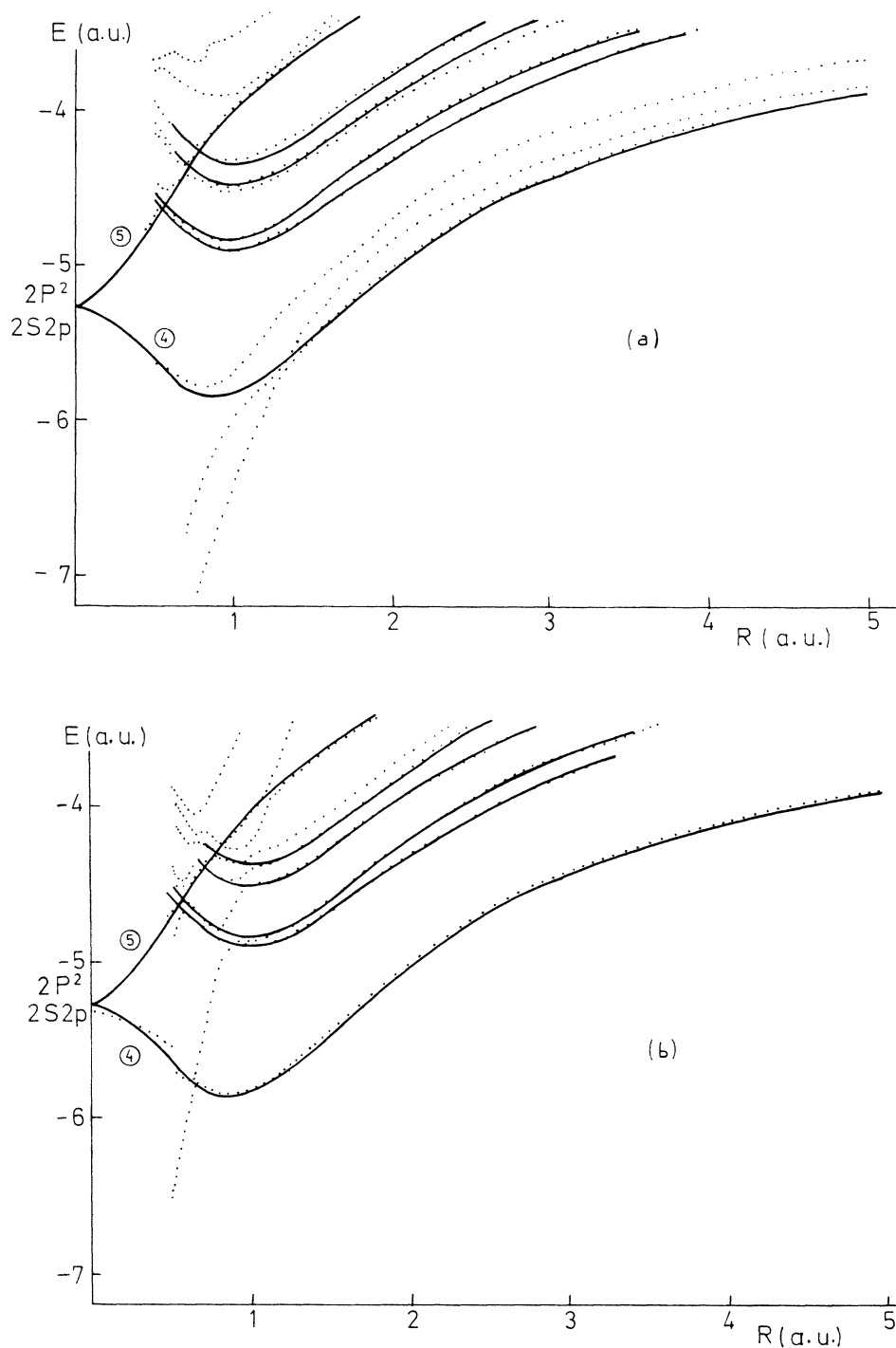


FIG. 4. Same as Fig. 3 for ${}^1\Pi$ states. The crossing between these states in the qualitative correlation diagram does not show since the U.A. limits ${}^1\Pi(2s2p)$ and ${}^1\Pi(2p^2)$ are practically degenerate. Basis sets of Tables I and III. Labels 4 and 5 correspond to ${}^1\Pi$ states appearing in Fig. 1. (a) Scaling parameter $\beta = 1.0$; (b) $\beta = 4.0$.

with origin on the center of nuclear charge. The energies of these wave functions cross as in the diagram of Fig. 1, instead of avoid crossing as do the adiabatic energies, but these avoided crossings are so narrow as to be crossed diabatically during the collision, except at very low impact velocities. Hence, for $R < 0.5$ a.u., those wave functions are better suited to represent the collision process than the adiabatic ones.

A feature that is apparent from Fig. 3(a) is that the molecular state that correlates diabatically to the entrance channel $\text{Li}^{3+} + \text{He}(1s^2)$ for $R \rightarrow \infty$ and to the autoionizing $2p^2$ state of the united-atom B^{3+} for $R \rightarrow 0$, becomes physically stable for a range of internuclear distances $0.9 \text{ a.u.} \lesssim R \lesssim 2.8 \text{ a.u.}$ It should be remarked, however, that for this range of distances, the exact Born-Oppenheimer eigenenergy presents an infinity of avoided crossings with

TABLE I. Exponents of the Gaussian orbitals used in the molecular calculations for $0.5 < R < 5.0$ a.u.

Li		He	
Σ states			
α_s	α_{2p_z}	α_s	α_{2p_z}
0.20	0.32	0.20	0.32
1.60	2.00	1.20	1.28
12.80	12.00	7.20	5.12
100.00		43.20	
Π states			
α_s	α_{2p_x}	α_s	α_{2p_x}
0.10	0.01	0.30	0.05
0.50	0.04	0.70	0.25
1.50	0.10	1.70	1.25
5.00	0.30	4.00	
16.00	1.00	10.00	
55.00	3.00	30.00	

the energies of the members of the two Rydberg series:

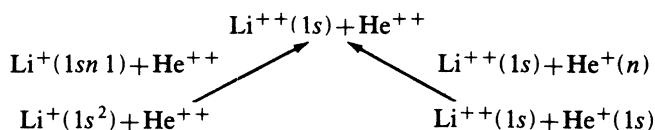


TABLE II. Exponents of the Gaussian orbitals (to reproduce the exact separated-atom atomic orbitals we have added to a GTO basis adequately scaled STO-3G contractions taken from Ref. 20) used in the molecular calculations for $R > 5.0$ a.u.

Li		He	
Σ states			
ψ_s		ψ_{2p_z}	ψ_s ψ_{2p_z}
0.005		0.08	0.030 0.080
0.025		0.3	0.100 2.000
0.100	(0.391 96)0.1690 + (0.607 68)0.5198 + (0.155 92)2.2370		0.300
0.600			1.000
3.000			3.500
15.000			13.000
(0.444 64)2.2471 + (0.535 33)0.9131 + (0.154 33)5.0123 ^a			
(0.700 11)0.1690 + (0.399 51)0.5198 - (0.099 97)2.2370			
Π states			
ψ_s		ψ_{2p_x}	ψ_s ψ_{2p_z}
0.005		0.080	0.030 0.001
0.025		0.300	0.100 0.005
0.100		1.200	0.300 0.025
0.600		5.000	3.500 0.125
3.000	(0.391 96)0.1690 + (0.607 68)0.5198 + (0.155 92)2.2370 ^a		13.000 0.600
15.000			3.000
54.000			15.000
(0.444 64)2.2471 + (0.535 33)0.9131 + (0.154 33)5.0123 ^a			
(0.700 11)0.1690 + (0.399 51)0.5198 - (0.099 97)2.2370			

^aWe have used the following abbreviations: $\sum(c)\alpha$ stands for $\sum_i c_i e^{-\alpha_i r^2}$ for ψ_s , $\sum_i c_i z e^{-\alpha_i r^2}$ for ψ_{2p_z} , and $\sum_i c_i x e^{-\alpha_i r^2}$ for ψ_{2p_x} .

converging to LiHe^{4+} . Since for our basis sets, Rydberg states turn out to be just as unstable as continuum ones, the stabilization approach then yields a diabatic state whose energy crosses that of the Rydberg series in the region where it becomes stable and whose (electrostatic) couplings with that series will be ineffective in the energy range considered. Hence, this wave function (as constructed by stabilization) is precisely the one needed²¹ in order to treat the collision process.

Taking the optimum values of $\beta=2$ (corresponding to the region where the eigenvalues are most stable) we obtain the following differences between the stabilized eigenvalues and the corresponding ones obtained by block diagonalization: for $R=5$ a.u. these differences are 0.01, 0.04, and 0.05 % for the first three $^1\Sigma$ resonances, respectively; at $R=0.5$ a.u. the corresponding values are 0.15, 0.30, and 0.70 %; therefore the results from the three representations join very smoothly. No other *ab initio* calculations have been performed on LiHe^{3+} , and comparison with previous work is not possible. On the other hand, it is interesting to compare our *energy differences* with those of Casaubón *et al.*¹² The most physically transparent way to do this is to assume, as in the one-electron diatomic molecule (OEDM) method of Harel and Salin,²² that one electron occupies an "inner" $2p\sigma$ orbital of LiHe^{4+} , while the other electron occupies an "outer" orbital of the screened nuclei, that depends upon the molecular state in question. This assignment would completely agree with the MO picture used in our Fig. 1, with the inner and outer orbitals drawn below and above the corresponding

TABLE III. Exponents of the Gaussian orbitals used in the molecular calculation for $R \leq 0.5$ a.u. One center expansion with origin at the center of nuclear charge.

Σ states	Π states
$\alpha_s \alpha_{2p_z}$	$\alpha_s \alpha_{2p_x}$
0.05	0.15
0.15	0.35
0.45	0.65
1.35	1.15
4.00	2.25
12.00	4.55
36.00	9.05

energy curves, respectively. In the one-electron model the interaction between inner and outer electrons is not neglected, as it would be in an independent electron model, but taken into account through an effective potential; whether it is correctly taken into account is precisely the question we seek to answer. If we add to the results of Ref. 12 the energy of the first excited $2p\sigma$ state of LiHe^{4+} which corresponds to the inner orbital in Fig. 1, we should obtain results which are comparable to ours. Indeed, the agreement between both sets of data, presented in Table IV, shows the correctness of our picture, and of both sets of calculations.

The radial couplings between the molecular states of

Table IV were calculated analytically by the method of Macías and Riera,²³ and are presented in Fig. 5 and Table V, with the origin of electronic coordinates on the lithium nucleus, for one value of the stabilization parameter $\beta=2.0$, and for the range of internuclear distances ($2.0 < R < 9.0$ a.u.) that is important in the dynamics of $\text{Li}^{3+} + \text{He}$ collisions. We have thus excluded the extremely high (≈ 148 a.u.) radial coupling that corresponds to the sharp avoided crossing between E_2 and E_3 at $R \approx 8.8$ a.u. This particular avoided crossing (shown as the farthest crossing in the schematic diagram of Fig. 1) will be traversed diabatically during the collision, and can therefore be diabaticized in the treatment of the process. This diabaticization has been performed in Table IV.

The most conspicuous feature of Fig. 5 is the appearance of a Lorentzian sharp peak for the $1^1\Sigma-2^1\Sigma$ coupling at $R \approx 7.8$ a.u. (which has very similar characteristics to the $2^1\Sigma-3^1\Sigma$ peak discussed above) and it is precisely the one taken into account in the Landau-Zener treatment of Stollberg and Lee.⁸ For the nuclear velocities considered by Wirkner-Bott *et al.*⁴ it is ineffective in the collision process and it can be diabaticized. However for $R < 7.8$ a.u. the $1^1\Sigma-2^1\Sigma$ coupling presents an exponential tail that is due to a delocalization of the corresponding electron clouds. As could be expected, this localization affects the bonding $\psi_2 = ||1S_{\text{He}}(2s + 2p_z)_{\text{Li}}||$ wave function rather than the antibonding one: $\psi_3 = ||1S_{\text{He}}(2s - 2p_z)_{\text{Li}}||$ (see Fig. 1).

TABLE IV. Molecular energies^a for singlet Σ and Π autoionizing states of the quasimolecule LiHe^{+3} .

R	Σ states			Π states	
	$-E_1$	$-E_2$	$-E_3$	$-E_4$	$-E_5$
0.4	5.9048 (5.9614) ^b	5.3414 (5.4263)	4.4000 (4.4815)	5.5200 (5.5655)	4.8500
0.5	6.1476	5.4148	4.5871	5.6100	4.6693
0.6	6.3788 (6.5231)	5.4907 (5.5886)	4.7503 (4.8261)	5.7200 (5.7798)	4.5700
0.7	6.6700	5.5570	4.8816	5.8230	4.3900
0.8	6.8230 (6.9011)	5.5998 (5.6966)	4.9729 (5.0514)	5.8520 (5.8991)	4.2572
0.9	6.8756	5.6151	5.0227	5.8501	4.1215
1.0	6.9075 (7.0212)	5.6034 (5.6939)	5.0335 (5.1182)	5.8209 (5.8970)	4.0022
1.5	6.4850	5.2949	4.7899	5.4501	3.5821
2.0	5.8550 (5.9231)	4.9039 (4.9500)	4.5759 (4.7470)	5.0179 (5.0730)	3.2862
2.5	5.3259 (5.3668)	4.5738 (4.6122)	4.4197 (4.5648)	4.6782 (4.7042)	3.0854
3.0	4.9338 (4.9554)	4.3387 (4.4076)	4.2947 (4.3704)	4.4303 (4.4408)	2.9280
3.5	4.6360	4.1892	4.1648	4.2500	2.7900
4.0	4.4053 (4.4198)	4.0600 (4.1471)	4.0500 (4.0623)	4.1092 (4.1052)	2.6510
4.5	4.2246 (4.2414)	4.0002 (4.0514)	3.9333 (3.9685)	4.0097 (3.9956)	2.5520
5.0	4.0810 (4.1004)	3.9175 (3.9507)	3.8512 (3.8765)	3.9136 (3.9068)	2.4489
6.0	3.8722 (3.8929)	3.8012 (3.8075)	3.7476 (3.7518)		
7.0	3.7262 (3.7473)	3.6997 (3.7036)	3.6587 (3.6622)		
8.0	3.6240 (3.6263)	3.6171 (3.6391)	3.5913 (3.5946)		
9.0	3.5644 (3.5668)	3.5350 (3.5511)	3.5380 (3.5418)		
10.0	3.5173 (3.5195)	3.4669 (3.4882)	3.4963 (3.4994)		
12.0	3.4473 (3.4494)	3.3667 (3.3880)	3.4323 (3.4354)		
14.0	3.3978 (3.3997)	3.2952 (3.3165)	3.3863 (3.3895)		
16.0	3.3609	3.2416	3.3516		
18.0	3.3324	3.1999	3.3244		
20.0	3.3097	3.1666	3.2026		
40.0	3.2086	3.0166	3.2016		

^aAs indicated in text the $2^1\Sigma-3^1\Sigma$ sharp avoided crossing at $R \approx 8.8$ a.u. has been diabaticized.

^bComparison with the results of Ref. 12, transformed as indicated in text, is afforded by the numbers between brackets. The agreement between both sets of data confirms the validity of both approaches and the physical basis behind the correlation rules of Fig. 1.

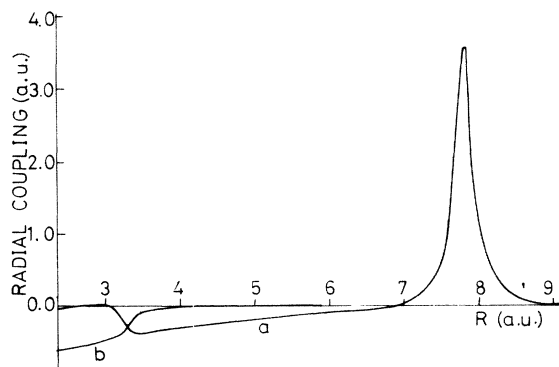


FIG. 5. Radial coupling between (a) $1^1\Sigma$ and $2^1\Sigma$ states; (b) $1^1\Sigma$ and $3^1\Sigma$ states. The arrow indicates the position of the extremely high (≈ 148 a.u.) peak that arises from the sharp avoided crossing between these states and which has been diabaticized.

Accordingly, the $1^1\Sigma$ - $2^1\Sigma$ radial coupling is much greater than the $1^1\Sigma$ - $3^1\Sigma$ one, for $R > 3$ a.u. For still smaller internuclear distances, the bonding state smoothly correlates (see Fig. 1) to the united-atom $2p3p$ state, while the antibonding wave function ψ_3 correlates to $2s2p$. Since the noncrossing rule applies, there exists, at $R \approx 3.25$ a.u., a sharp avoided crossing between E_2 and E_3 , where the corresponding wave functions exchange their character. Then, for $R < 3.2$ a.u., the $1^1\Sigma$ - $3^1\Sigma$ d/dR matrix element becomes larger than the $1^1\Sigma$ - $2^1\Sigma$ one.

TABLE V. Radial coupling matrix elements between $^1\Sigma$ states. Origin on lithium nucleus.

R	$1^1\Sigma$ - $2^1\Sigma$	$1^1\Sigma$ - $3^1\Sigma$
2.0	-0.1450	-0.6937
2.2	-0.1147	-0.6444
2.4	-0.0615	-0.6097
2.5	-0.0462	-0.5939
2.6	-0.0322	-0.5712
2.8	-0.0060	-0.5260
3.0	-0.0279	-0.4825
3.1	-0.0596	-0.4596
3.2	-0.1307	-0.4249
3.3	-0.2963	-0.3070
3.4	-0.3774	-0.1596
3.6	-0.3705	-0.0765
3.8	-0.3459	-0.0527
4.0	-0.3210	-0.0407
4.2	-0.2973	-0.0327
4.4	-0.2746	-0.0267
4.6	-0.2528	-0.0220
4.8	-0.2318	-0.0184
5.0	-0.2116	-0.0156
6.0	-0.1043	-0.0038
7.0	0.0344	-0.0018
7.5	0.5763	0.0020
7.6	1.1070	
7.7	2.3122	
7.8	3.5815	
7.9	2.3689	
8.0	1.1460	0.0045
9.0	0.0277	0.0589

The physical situation that gives rise to the avoided crossing between E_2 and E_3 at $R \approx 3.25$ a.u. has been studied in detail by Eichler *et al.*²⁴ and by Falcon *et al.*²⁵ Notice, however, that the situation here is slightly different; the d/dR Lorentzian peak is only a consequence of the interchange of character at the pseudocrossing and does not present any Stark coupling contribution (neither the peak nor the tail). The reason for the difference is simply that the asymptotic form of the Li^{2+} ($n=2$) orbitals is precisely that of the Stark hybrids $(2s+2p)_{Li}$; hence, in the present case there is no Stark coupling because the exit channel corresponds to hydrogenlike atoms. Correspondingly, the coupling at the pseudocrossing has an area $\pi/2$, and it can be trivially diabaticized, and then ignored. Paradoxically, we have found that precisely the case of sharp avoided crossings which are irrelevant, as the previous one, to the dynamics of the process, is difficult to treat correctly by the stabilization method; in fact this was another good reason to choose the VB-BD procedure (without stabilization) for $R > 5$ a.u. in our calculations. The reason for this difficulty is that the exact position and height of the sharp d/dR matrix element turns out to be much more sensitive to the scaling parameter β than its area (which is always $\pi/2$, as befits a complete interchange of character between the wave functions). Furthermore, one can even obtain avoided crossings between the energy curves, for a fixed internuclear distance, as functions of β . We illustrate the difficulty in stabilizing very sharp radial couplings at pseudocrossing in Fig. 6 where we plot calculated values of the $2^1\Sigma$ - $3^1\Sigma$ coupling for two values of β . In the present application it is fortunate that this shortcoming of the stabilization method in the calculation of radial couplings—which to our knowledge has never been mentioned before—is not important. However, this need not be so at low impact energies, and it constitutes a liability of the stabilization method to calculate radial couplings. On the other hand,

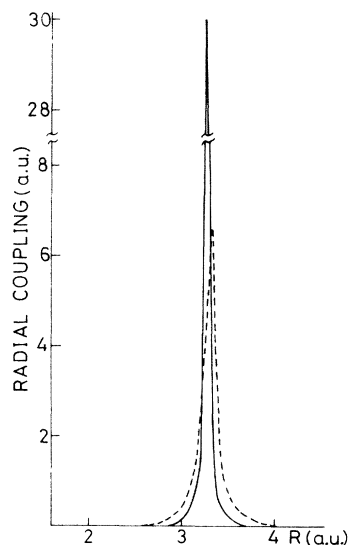


FIG. 6. Radial coupling between 2^1 - 3^1 states for two choices of the scaling parameter in Eq. (1): —, $\beta=2$; - - -, $\beta=2.4$.

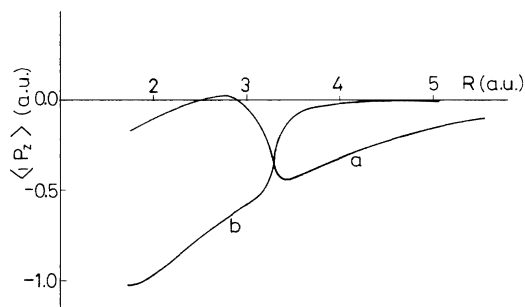


FIG. 7. Matrix elements of iP_z which yield the origin dependence of radial couplings presented in Fig. 5. Notice the different scales of both figures.

the computation of couplings which should be accurately known to treat the $\text{Li}^{3+} + \text{He}$ collision for $E > 2$ keV presents no such problems. The stabilization pattern for these couplings is similar to the one presented in Fig. 2 for the energies, and is not shown for the sake of conciseness.

As a consequence of the previous reasonings, it appears that, apart from the effect of rotational couplings, the only mechanism which can explain the high values for the measured charge-exchange cross section⁴ occurs through the delocalization tail of the $1^1\Sigma-2^1\Sigma$ coupling, discussed above, which is well calculated by our method. On the other hand, this coupling turns out to be strongly origin dependent; we show in Fig. 7 the values of the terms that yield²³ this origin dependence, which are the matrix elements of iP_z , where P_z is the component of the electronic linear momentum along the internuclear axis.

To illustrate the consequences of that origin dependence it is sufficient to perform a two-by-two calculation involving the delocalization tail. The total cross sections calculated using the program PAMPA,²⁶ in the velocity range 0.1 to 0.7 a.u., with the origin of electronic coordinates either on the Li or on the He nucleus, differ by about a factor of ~ 3 , and they also strongly depend on the values of that radial coupling for R between 4 and 8 a.u. This clearly shows that a collisional treatment without translation factors (TF) would be of doubtful value,^{13,27} and that both energies and radial couplings must be accurately determined in that region of internuclear distances. A related additional problem, in the present case, is the choice of the translation factor (or of the parameters in this fac-

tor), in the R range, where effective transitions take place. Inclusion of TF will modify both the energies and radial couplings, and these modifications—in the same region—will depend, in general, on the choice of parameters. Consequently, the sensitivity of the calculated charge-exchange cross section to that choice of parameters can be, in the present case, as important as the origin dependence of the results when no translation factors are used.² As a conclusion, a (time-consuming) optimization procedure²⁸ seems necessary, since there is no *a priori* rigorous and simple criteria to choose the translation factors.

IV. FINAL REMARKS

The aim of this paper was to present for the first time a detailed application of the stabilization method to the calculation of energy correlation diagrams and of the corresponding radial couplings between states lying in the ionization continuum. Using the quasimolecule LiHe^{3+} as an example, we show that qualitative correlation diagrams and the rule of smoothest topological correlation can be used for autoionizing states just as for ordinary bound ones. Furthermore, we exemplified how CI techniques can be applied to calculate these molecular properties (energies and radial couplings) for autoionizing states, without modification of standard computer programs.

Finally, we have pointed out that, just as for molecular energies, radial couplings also stabilize, except for the special case of very sharp avoided crossings; the method is therefore not very well suited for the treatment of collisions that take place at very low impact energies, and this is also a new conclusion.

For the particular case of the LiHe^{3+} system in the ionization continuum, used to discuss the previous points, we have found that the most effective ($1^1\Sigma-2^1\Sigma$) radial coupling is so strongly origin dependent that (probably optimized) TF must be included to calculate cross sections; this is a nontrivial problem which will be the object of future work.

ACKNOWLEDGMENTS

All calculations were performed at the Universidad Autónoma de Madrid IBM/UAM and Centro de Calculo (CC)/UAM Centers, Madrid, Spain.

*Also at Consejo Superior de Investigaciones Científicas, Madrid.

¹A. Macías, A. Riera, and M. Yáñez, *Phys. Rev. A* **23**, 2941 (1981); **27**, 206 (1983); **27**, 213 (1983).

²L. F. Errea, L. Méndez, and A. Riera, *Phys. Rev. A* **27**, 3357 (1983).

³F. Borondo, A. Macías, and A. Riera, *Phys. Rev. Lett.* **46**, 420 (1981); *J. Chem. Phys.* **74**, 6126 (1981); *Chem. Phys.* **81**, 303 (1983).

⁴S. K. Allison, J. Cuevas, and M. García Muñoz, *Phys. Rev.* **120**, 1266 (1960); V. S. Nikolaev, L. N. Fateeva, I. S. Dimi-

triev, and Ya. A. Teplova, *Zh. Eksp. Teor. Fiz.* **40**, 989 (1961) [*Sov. Phys.—JETP* **13**, 695 (1961)]; L. I. Pirovar, Yu. Z. Levchenko, and G. A. Krisvosonov, *Zh. Eksp. Teor. Fiz.* **59**, 19 (1970) [*Sov. Phys.—JETP* **32**, 11 (1971)]; M. B. Shah, T. W. Goffe, and H. B. Gilbody, *J. Phys. B* **11**, L233 (1978); I. Wirkner-Bott, W. Seim, A. Muller, P. Kester, and E. Salzborn, *ibid.* **14**, 3987 (1981).

⁵A. V. Vinogradov and I. I. Sobelman, *Zh. Eksp. Teor. Fiz.* **63**, 2113 (1972) [*Sov. Phys.—JETP* **36**, 1115 (1973)]; M. O. Skully, W. H. Louisell, and W. B. McKnight, *Opt. Comm.* **9**, 246 (1973); W. H. Louisell, M. O. Skully, and W. B. McKnight,

- Phys. Rev. A **11**, 989 (1975).
- ⁶H. S. Taylor, Adv. Chem. Phys. **18**, 91 (1970).
- ⁷A. Macías and A. Riera, J. Phys. **46**, 535 (1985).
- ⁸M. T. Stollberg and H. W. Lee, Phys. Rev. A **29**, 2448 (1984).
- ⁹H. Suzuki, Y. Kajitawa, W. Toshima, H. Ryufuku, and T. Watanabe, Phys. Rev. A **29**, 525 (1984).
- ¹⁰H. Ryufuku and T. Watanabe, Phys. Rev. A **28**, 2005 (1978).
- ¹¹See, for example, R. K. Janev and B. H. Bransden, International Atomic Energy Agency Report No. INDC (NDS)-135/6A (International Atomic Energy Agency, Nuclear Data Section, Vienna, 1982), and references therein.
- ¹²J. I. Casaubón, C. Falcón, and L. Opradolce (unpublished).
- ¹³A. Macías and A. Riera, Phys. Rep. **90**, 299 (1982).
- ¹⁴M. Barat and W. Lichten, Phys. Rev. A **6**, 211 (1972).
- ¹⁵H. Sato and S. Hara, J. Phys. B **13**, 4577 (1980); **17**, 4301 (1984).
- ¹⁶N. Moiseyev and F. Weinhold, Phys. Rev. A **20**, 27 (1979).
- ¹⁷A. Macías and A. Riera, Chem. Phys. Lett. **117**, 42 (1985).
- ¹⁸W. H. Miller and H. Morgner, J. Chem. Phys. **67**, 4923 (1977); R. D. Taylor and J. B. Delos, Proc. R. Soc. London, Ser. A **379**, 179 (1982).
- ¹⁹A. Macías, R. Mendizábal, F. Pelayo, A. Riera, and M. Yáñez, J. Mol. Struct. Theochem. **107**, 245 (1984).
- ²⁰W. J. Hehre, R. F. Stewart, and J. A. Pople, J. Chem. Phys. **51**, 2657 (1969).
- ²¹W. Lichten, Phys. Rev. **139**, 27 (1965); **164**, 131 (1967).
- ²²C. Harel and A. Salin, J. Phys. B **13**, 785 (1980); **16**, 55 (1983).
- ²³A. Macías and A. Riera, J. Phys. B **10**, 861 (1977); **11**, 1077 (1978).
- ²⁴J. Eichler, U. Wille, B. Fastrup, and K. Taulbjerg, Phys. Rev. A **14**, 767 (1976).
- ²⁵C. Falcon, A. Macías, A. Riera, and A. Salin, J. Phys. B **14**, 1973 (1981).
- ²⁶C. Gaussorgues, R. D. Piacentini, and A. Salin, Comput. Phys. Commun. **10**, 233 (1975).
- ²⁷K. Taulbjerg and T. S. Briggs, J. Phys. B **8**, 1895 (1975); **8**, 1641 (1975); W. R. Thorson and J. B. Delos, Phys. Rev. A **18**, 117 (1978); **18**, 135 (1978).
- ²⁸See, for example, T. A. Green, J. C. Browne, H. H. Michael, and M. M. Madsen, J. Chem. Phys. **61**, 5198 (1974); **61**, 5186 (1974); **69**, 101 (1978); J. Rankin and W. R. Thorson, Phys. Rev. A **18**, 1990 (1978); A. Riera, *ibid.* **30**, 2304 (1984), and references therein.